Fabrication of polynomial 3-D nanostructures in Si with a single-step process

Dong Liu,[a] Shakib Morshed,[a] Bo Zhou,[a] Barton C. Prorok,[a] and Soo-Young Lee[b]
[a]Auburn University, Materials Research and Education Center, 275 Wilmore Lab, Auburn, Alabama 36849–5341
[b]Auburn University, Department of Electrical and Computer Engineering, 200 Broun Hall, Auburn, Alabama 36849–5201
E-mail: prorok@auburn.edu

Abstract. This work demonstrated the ability to transfer a nanoscale 3-D polynomial structure of arbitrary shape into Si with a single step electron-beam lithography process. The technique involved employing a proximity correction algorithm, PYRAMID, to derive the dose distribution for a given 3-D structure by accounting for the electron scattering effects of the surrounding pixels. The pattern was written into a polymethyl methacrylate (PMMA) resist and then successively transferred into Si via reactive ion etching, where a 1:1 etching ratio between PMMA and Si was achieved. The pattern transferred into Si possessed nanoscale features and matched the desired pattern with high fidelity. [DOI: 10.1117/1.3563601]

Subject terms: 3-D nanolithography; single-step lithography; proximity correction.

Paper 09155LR received Nov. 11, 2010; revised manuscript received Jan. 5, 2011; accepted for publication Feb. 4, 2011; published online Mar. 29, 2011.

1 Introduction

There are numerous electronic devices that utilize 3-D structures of various shapes, such as arrays of particles, gratings, photonic band gap crystal, magnetoresistive random access memory (MRAM), and nanoelectromechanical systems (NEMS). The properties of these structures show high sensitivity to their dimensional characteristics such as shape, size, etc., which often results in enhanced functionality. As the feature size in these 3-D structures is decreased toward the nanoscale, it becomes more and more challenging to achieve high dimensional accuracy and reliability in their fabrication. Thus, there is a growing need for improving how accurately and reliably these 3-D structures are fabricated.

Various approaches have been proposed and employed in an attempt to fabricate 3-D structures possessing nanoscale features. They include plasma etching,[1] electrodeposition with a special patterning and biasing of the seed layer,[2] direct and laser-assisted chemical etching,[3] ultrasonic machining,[4] electro-discharge machining,[5] layer-by-layer laser-induced polymerization,[6] nanoimprint lithography,[7,8] hole-area modulation,[9] local nanolithography by atomic force microscopy (AFM),[10] parallel nano-oxidation,[11] etc. However, critical drawbacks to many of these methods include that they are designed for only a few specific shapes, are limited in speed for industrial fabrication, or require unconventional equipment or tools. Electron-beam (e-beam) lithography is a prime candidate for fabricating grayscale structures of nanoscale since it can achieve high spatial resolution and has the flexibility to handle various general shapes.[12,13] One possible approach is to employ binary e-beam lithography, which involves multiple lithographic processes, one for each discrete depth. This approach requires a long processing time, is susceptible to alignment error, and would require an impractically large number of lithographic processes to obtain grayscale structures with smooth surfaces. Grayscale (e-beam and optical) lithography avoids such drawbacks, requiring a single step of lithographic process. However, the 3-D structures fabricated in the past were of regular shape.[14–19] Also, the feature size was relatively large, well above 1 μm. In this work, grayscale e-beam lithography is employed in order to fabricate 3-D structures with a smooth surface of arbitrary shape and the feature size below 1 μm by a single lithographic process. It takes advantage of blurring due to the proximity effect, caused by electron scattering in the resist, to achieve the smooth contour. The results in this paper not only demonstrate such ability but also have a potential to trigger development of devices with nontraditional 3-D structures.

2 Experimental Details

2.1 *Polynomial Structure*

The PYRAMID[17,18,20,21] software was used to compute the exposure distribution for the polynomial structure. One of the main functionalities of the PYRAMID software includes derivation of the dose distribution given an exposure distribution or vice versa. PYRAMID adopts a space-invariant linear system model of the lithographic process and estimates exposure by the convolution between a dose distribution and a point spread function (PSF). The PSF depicts the energy (exposure) distribution in the resist when a point is exposed. A distinct feature of the PYRAMID approach, compared to others, is that it distinguishes the short-range electron scattering from the long-range during convolution. This enables PYRAMID to find the exposure distribution in a pattern quickly and accurately.

The target polynomial pattern is shown in Fig. 1, which may be represented by $f(x,y) = p(x)$ where $p(x)$ is a fourth order polynomial. It was designed to possess smooth surfaces of arbitrary shape rather than discrete levels and sharp transitions. The shape has a maximum depth of approximately 60 nm with two separate smooth, nanoscale furrow features. The pattern width was chosen to be 2.5 μm to avoid any mass transfer issues in the Si etching processes. Since there are two valleys and one peak in the polynomial structure (see Fig. 1), the feature size can be considered to be $2.5/3 \approx 0.83$ μm. The domain (x,y) of the pattern was partitioned in the x dimension into 25 thin rectangles of 100 nm $\times$ 10 μm each where a dose is assigned to each rectangle.

The target exposure distribution was derived by sampling $p(x)$ at the interval of 100 nm, i.e., it is linearly proportional to $p(x)$. Then, the PYRAMID software was used to compute the dose distribution, shown in Fig. 2(a), required to achieve the exposure distribution. The actual exposure distribution

1932-5150/2011/$25.00 © 2011 SPIE

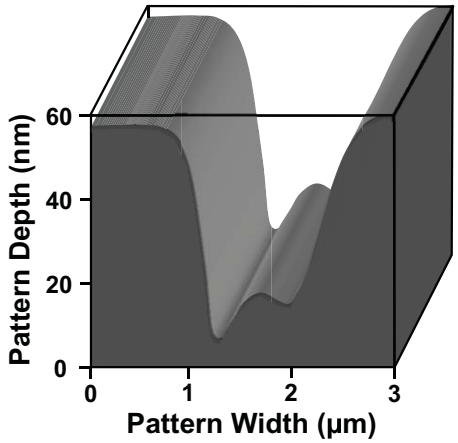

Fig. 1 Schematic representation of the target polynomial structure.

estimated by the PYRAMID software is shown in Fig. 2(b). Though the (estimated) exposure distribution shows discrete levels, the resulting resist profile would be smooth due to the proximity effect and isotropic nature of the developing process.

2.2 *Fabrication and Characterization*

Polymethyl methacrylate (PMMA) 950K resist was chosen to imprint the desired pattern in a (100) Si wafer. The process began first with cleaning the wafer with acetone (30 s), followed by alcohol (30 s), rinsing with de-ionized water (1 min), and then dehydration at 120 °C for 90 min. The polymethyl methacrylate (PMMA) resist was then spun on using a speed of 6000 rpm for 45 s to achieve a thickness of approximately 100 nm. The wafer was then baked at 180 °C for 5 min to evaporate the solvent. The thickness of the PMMA resist after the spin-coating was confirmed with a calibrated ellipsometer. The e-beam lithography was performed at 30 kV on a JEOL 7000 F field-emission electron microscope with an integrated Nabity NPGS-60 nanometer pattern generation system.

The dose distribution in Fig. 2(b) was imported into the NPGS and written into the PMMA resist. After exposure, the samples were developed at room temperature in an ultrasonic bath using an MIBK:IPA = 1:3 developer for 115 s. This was followed by rinsing with methanol and then blow drying with pure N_2 gas. The structures generated in the resist were characterized by AFM with cantilevers possessing a vertical resolution of 10 nm. Reactive ion etching (RIE)[22] was employed to transfer the pattern from PMMA resist

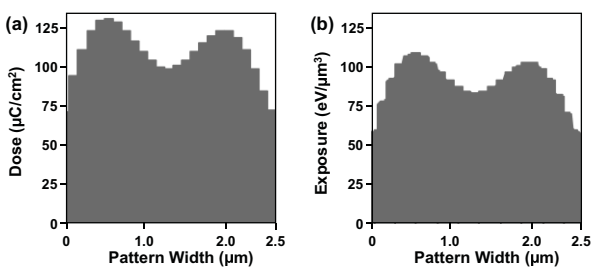

Fig. 2 (a) Dose distribution and (b) estimated exposure distribution.

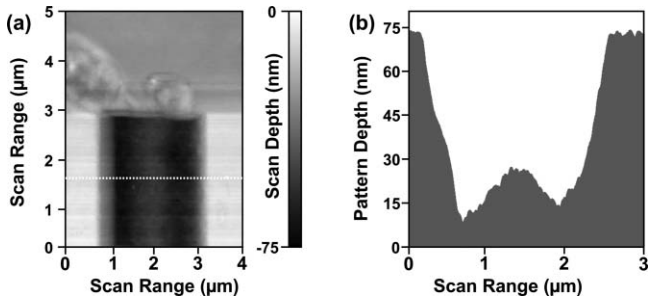

Fig. 3 AFM scan of the pattern imprinted into the PMMA resist: (a) top-view and (b) vertical cross-section at dashed line.

to the Si wafer. The plasma etching was performed under 600 W of power in an SF_6/O_2 gas mixture with a flow ratio 10:1. Following etching, the samples were immediately cleaned with acetone and methanol to remove any residual material. The polynomial structures in the Si were then characterized by AFM.

3 Results and Discussion

After exposing and developing the PMMA resist, the geometry of the pattern was characterized by AFM. Figure 3(a) is the scan of the pattern and Fig. 3(b) is a vertical cross-section taken at the dashed line. The measured height and width of the entire polynomial structure pattern were 63.2 nm and 2.56 μm, respectively. The surface of the polynomial structure and surrounding PMMA was not ideally smooth, possessing a degree of surface roughness, root mean square of 2.52 nm. This roughness is likely a result of nonideal nanotransport of solvent and solute into the polymer, which can result in less-defined and swollen features. Others researchers have characterized this phenomenon and demonstrated that it can be minimized by employing a higher molecular weight PMMA and ultrasonic-aided development of PMMA.[23] This work leveraged these techniques and obtained a rather low surface roughness, which was approximately 20 to 30 times less than the desired pattern features. As will be shown in the following results, this roughness appeared to have only a negligible influence on transferring the pattern into Si.

After transferring the polynomial pattern into Si via RIE, AFM characterization was performed (see Fig. 4). The cross-sectional slice of the pattern indicates that the shape was successfully transferred into the Si substrate. The pattern depth and width of the polynomial structure were measured

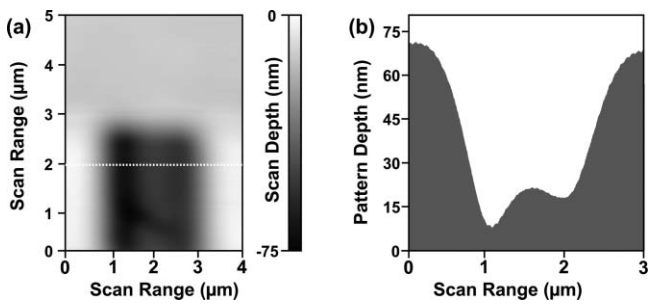

Fig. 4 AFM scan of the pattern transferred into Si substrate: (a) top-view and (b) vertical cross-section at the dashed line.

to be 58.2 nm and 2.71 μm, respectively, and matches the dimensions of the desired pattern well. The pattern profile is smoother and more uniform than that of the resist, likely due to the isotropic characteristics of fluorine-based Si etching.[24] Thus, the roughness resulting from the developing process had little to no effect on the etched pattern. Finally, the chosen etching parameters resulted in an approximate 1:1 etching rate between the PMMA resist and Si substrate. This is highly desired as maintaining the resist profile as close to the desired 3-D structure as possible and enables simplification of the pattern generation and transfer by RIE etching. To our knowledge, no other published works have demonstrated the ability to fabricate nanoscale 3-D structures of arbitrary shape using grayscale electron-beam lithography in a single step.

4 Summary

Using grayscale electron-beam lithography along with dose computation and exposure simulation by the PYRAMID software, a 3-D polynomial nanostructure of arbitrary shape was imprinted in PMMA on Si by a single lithographic step. This shape was successfully transferred into a Si substrate using RIE while achieving a 1:1 etching ratio between PMMA and Si. These results demonstrate the ability to fabricate a 3-D polynomial nanostructure into a substrate with good fidelity by a single-step lithographic process.

Acknowledgments

This work was supported by the U.S. National Science Foundation, Engineering Directorate, Civil and Mechanical Systems Program, under Contract No. CMMI-0709224.

References

1. M. Eisner and J. Schwider, "Transferring resist microlenses into silicon by reactive ion etching," *Opt. Eng.* **35**(10), 2979–2982 (1996).
2. A. Macissek, "Electrodeposition of 3D microstructures without molds," *Proc. SPIE* **2879** 275–279 (1996).
3. T. M. Bloomstein and D. J. Ehrlich, "Laser chemical three dimensional writing of multimaterial structures for microelectromechanics," *Proc. IEEE Conf. on Microelectromechanical Systems (MEMS'91), Nara*, Japan, pp. 202–203 (1991).
4. X. Q. Sun, T. Masuzawa, and M. Fujino, "Micro ultrasonic machining and its applications in MEMS," *Sens. Actuators, A* **57**(2), 15–164 (1996).
5. T. Masaki, K. Kawata, and T. Masuzawa, "Micro-electro-discharge machining and its applications to MEMS," *Proc. IEEE Conf. on Microelectromechanical Systems (MEMS'90),* pp. 21–26 (1990).
6. S. Zissi, A. Bertsch, J. Y. Jezequel, S. Corbel, D. J. Lourgnot, and J. C. Andre, "Stereolithography and microtechniques," *Microsyst. Technol.* **2**(1), 97–102 (1999).
7. S. Chou, P. Krauss, W. Zhang, L. Guo, and L. Zhuang, "Sub-10 nm imprint lithography and applications," *J. Vac. Sci. Tech. B* **15**(6), 2897–2904 (1997).
8. D. S. Macintyre, Y. Chen, D. Lim, and S. Thoms, "Fabrication of T gate structures by nanoimprint lithography," *J. Vac. Sci. Tech. B* **19**(6), 2797–2800 (2001).
9. T. Bourouina, T. Masuzawa, and H. Fujita, "The MEMSNAS process: microloading effect for micromachining 3-D structures of nearly all shapes," *J. Microelectromech. Syst.* **13**(2), 190–199 (2004).
10. J. Martinez, R. V. Martinez, and R. Garcia, "Silicon nanowire transistors with a channel width of 4 nm fabricated by atomic force microscope nanolithography," *Nano Lett.* **8**(11), 3636–3639 (2008).
11. J. Martinez, N. S. Losilla, F. Biscarini, G. Schmidt, T. Borzenko, L. W. Molenkamp, and R. Garcia, "Development of a parallel local oxidation nanolithography instrument," *Rev. Sci. Inst.* **77**(8), 086106 (2006).
12. E. Kuramochi, M. Notomi, T. Tamamura, T. Kawashima, S. Kawakami, J. Takahashi, and C. Takahashi, "Drilled alternating-layer structure for three-dimensional photonic crystals with a full band gap," *J. Vac. Sci. Tech. B* **18**(6), 3510–3513 (2000).
13. S. Y. Lin and J. Fleming, "A three-dimensional optical photonic crystal," *IEEE J. Lightwave Tech.* **17**(11), 1944–1947 (1999).
14. B. Morgan, C. Waits, J. Krizmanic, and R. Ghodssi, "Development of a deep silicon phase Fresnel lens using gray-scale lithography and deep reactive ion etching," *J. Microelectromech. Syst.* **13**(1), 113–120 (2004).
15. A. Sure, T. Dillon, J. Murakowski, C. Lin, D. Pustai, and D. Prather, "Fabrication and characterization of three-dimensional silicon tapers," *Opt. Express* **11**(26), 3555–3561 (2003).
16. R. Murali, D. Brown, K. Martin, and J. Meindl, "Process optimization and proximity effect correction for gray scale e-beam lithography," *J. Vac. Sci. Technol B* **24**(6), 2936–2939 (2006).
17. F. Hu and S.-Y. Lee, "Dose control for fabrication of grayscale structures using a single-step e-beam lithographic process," *J. Vac. Sci. Techol.. B* **21**(6), 2672–2679 (2003).
18. J. Kim, D. Joy, and S.-Y. Lee, "Controlling resist thickness and etech depth for fabrication of 3-D structure in electron-beam lithography," *Microelectron Eng.* **84**(12), 2859–2864 (2007).
19. V. A. Kudryashov, P. D. Prewett, and A. G. Michette, "A new e-beam method for grey scale 3D optical elements," *Microelectron. Eng.* **46**, 209–212 (1999).
20. S.-Y. Lee, J. C. Jacob, C. M. Chen, J. A. McMillan, and N. C. MacDonald, "Proximity effect correction in electron-beam lithography: a hierarchical, rule-based scheme – PYRAMID," *J. Vac. Sci. Technol. B* **9**(6), 3048–3053 (1991).
21. S. Y. Lee, "A flexible and efficient approach to proximity effect correction," *Surf. Interface Anal.* **37**(11), 919–926 (2005).
22. I. W. Rangelow, "Reactive ion etching for high aspect ratio silicon micromachining," *Surf. Coat. Technol.* **97**(1–3), 140–150 (1997).
23. D. G. Hasko, S. Yasin, and A. Mumtaz, "Influence of developer and development conditions on the behavior of high molecular weight electron beam resists," *J. Vac. Sci. Technol. B* **18**(6), 3441–3444 (2000).
24. S. M. Rossnagel, J. J. Cuomo, and W. D. Westwood, *Handbook of Plasma Processing Technology: Fundamentals, Etching, Deposition, and Surface Interactions*, Noyes Publications, New Jersey (1990).